

# Saturation of electrical resistivity in metals at large temperatures

M. Calandra and O. Gunnarsson  
*Max-Planck-Institut für Festkörperforschung D-70506 Stuttgart, Germany*

We present a microscopic model for systems showing resistivity saturation. An essentially exact quantum Monte-Carlo method is used to demonstrate that the model describes saturation. We give a simple explanation for saturation, using charge conservation and considering the limit where thermally excited phonons have destroyed the periodicity. A crucial feature of the model is that the atomic vibrations couple to the hopping matrix elements. We demonstrate the difference to a model where the vibrations couple to the level positions and where saturation does not happen.

In a metal, the electrical resistivity,  $\rho$ , grows with the temperature  $T$  due to the increased scattering of the electrons by phonons. Typically,  $\rho(T) \sim T$  for large  $T$ . For some metals with a very large  $\rho$ , however, the resistivity saturates [1–3], i.e., it grows very slowly with  $T$  for large  $T$ . The resistivity is often described in a semiclassical (Boltzmann) picture, where an electron, on the average, travels a mean free path  $l$  before it is scattered. The resistivity is inversely proportional to  $l$ . Typically,  $l \gg d$ , where  $d$  is the atomic separation. For systems with resistivity saturation, however,  $l$  becomes comparable to  $d$ . Work in the 1970’s suggested that resistivity saturation occurs universally when  $l \sim d$ , the Ioffe-Regel condition [4], providing an upper limit to the large  $T$  resistivity of metals. Later work has, however, found exceptions, such as alkali-doped fullerenes [5,6].

Intuitively, resistivity saturation seems natural. One might expect that at worst, an electron could be scattered at each atom, leading to  $l \sim d$ . Such a semiclassical picture, however, breaks down when  $l \sim d$  [7], and it is contradicted by the lack of saturation for fullerenes. Several theories of the resistivity saturation have been presented, usually based on generalisations of the semi-classical Boltzmann theory, but none has been generally accepted [8–10].

The Bloch-Boltzmann theory starts from a periodic system and treats the scattering mechanisms as small perturbations. Here we consider the opposite limit, where thermally excited phonons have removed all effects of periodicity. In this limit, charge conservation naturally leads to saturation for systems where the phonons couple to the hopping matrix elements. This happens to occur when  $l \sim d$ . We show, however, that this does not happen for systems where the phonons couple to the level positions. We first use an essentially exact quantum Monte-Carlo (QMC) calculation to demonstrate resistivity saturation in our model. We then introduce a method where the phonons are treated semiclassically and the electrons quantum-mechanically, justifying the method by comparing with the QMC results. This method is sufficiently simple to allow for an interpretation of the results.

Resistivity saturation is clearly observed for, e.g., A15 compounds, such as  $\text{Nb}_3\text{Sb}$  [1], while Nb metal only

shows weak saturation at large  $T$  [11]. We study a model  $\text{Nb}_3^*$  of  $\text{Nb}_3\text{Sb}$ , where the Nb atoms have the same positions as in  $\text{Nb}_3\text{Sb}$ , but the Sb atoms are neglected [12]. This model is compared with a model of Nb. We consider a cluster of  $N$  atoms, placed on the appropriate A15 ( $\text{Nb}_3^*$ ) or bcc (Nb) lattices with the lattice parameters 5.17 Å ( $\text{Nb}_3^*$ ) or 3.28 Å (Nb).

We study the scattering of the electrons from phonons. Each atom is assumed to have vibrations in the three coordinate directions, described by Einstein phonons. The phonon energy,  $\omega_{ph} = 14$  meV, is obtained from an average over the phonons of Nb [13]. For each Nb atom we include the five-fold degenerate ( $n = 5$ )  $d$ -orbital. The hopping matrix elements between the orbitals are obtained from Harrison [14], using a power dependence on the atomic distance  $d$  ( $\sim 1/d^m$ ). We use  $m = 3.6$  more appropriate for Nb [15] than  $m = 5$  used by Harrison. To avoid divergencies for very small  $d$ ,  $1/d^m$  is replaced by  $1/(d^m + a^m)$ , with  $a = 2$  Å. The vibrations of the atoms modulate the hopping matrix elements, both due to the changes of the atomic distances and the relative movements of the orbital lobes. We neglect the influence of the vibrations on the level energies. The Coulomb interaction between the electrons is also neglected. To obtain the resistivity, we calculate the current-current correlation function. The current operator  $\mathbf{j}$  is obtained by using charge and current conservation. Thus the matrix elements between orbitals  $\nu$  and  $\mu$  on sites  $\mathbf{R}^\nu$  and  $\mathbf{R}^\mu$  are

$$\mathbf{j}^{\nu\mu} = ie(\mathbf{R}^\nu - \mathbf{R}^\mu)t_{\nu\mu}, \quad (1)$$

where  $t_{\nu\mu}$  are the corresponding hopping matrix elements.

This model can be solved essentially exactly by using a determinantal quantum Monte-Carlo (QMC) method [16], treating the phonons quantum mechanically. For the models studied here, the QMC method has no “sign-problem”. The calculated correlation function (for imaginary time) therefore has only (small) statistical errors. We use a maximum entropy method [17] to obtain the optical conductivity  $\sigma(\omega)$  on the real frequency axis. The resistivity  $\rho$  is then  $1/\sigma(0)$ .

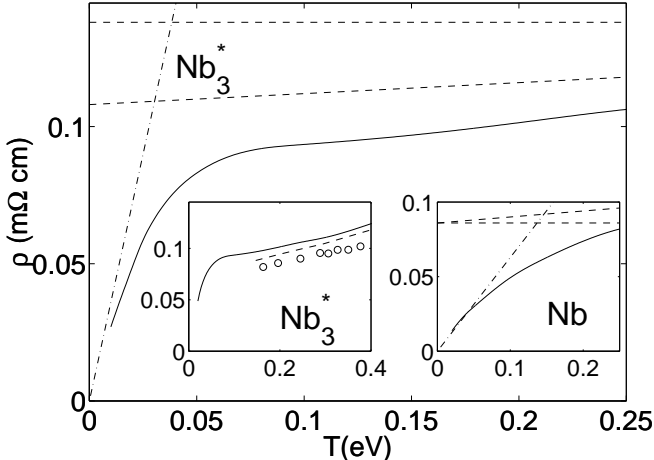


FIG. 1. Resistivity  $\rho(T)$  as a function of temperature  $T$ . The main figure shows results for  $\text{Nb}_3^*$  ( $N = 648$  atoms) and the right insert results for Nb ( $N = 640$  atoms), treating the phonons (semi)classically. The small  $T$  (Eq. (7)) (chain curves) and the two large  $T$  (Eq. (5), see text) limits of  $\rho(T)$  (broken curves) are also shown. The left insert compares the semiclassical (broken ( $N = 36$ ) and full ( $N = 648$ ) curves) and quantum Monte-Carlo (circles,  $N = 36$ ) calculations for  $\text{Nb}_3^*$ .

The left insert of Fig. 1 shows the QMC result (circles) for  $\rho(T)$  of the  $\text{Nb}_3^*$  model. We are particularly interested in the large  $T$  behaviour, which is also the limit where the QMC calculation can be performed with a reasonable effort. The large  $T$  result extrapolates to a substantial nonzero value. However, since the resistivity of the  $\text{Nb}_3^*$  model must go to zero for  $T = 0$ , the QMC calculation clearly shows that the model leads to a drastic reduction of the slope of the  $\rho(T)$  curve for large  $T$ , usually referred to as resistivity saturation.

To analyse the results, we treat the phonons (semi)classically. The atomic displacements due to the phonons are chosen randomly according to a Gaussian distribution, determined from the average number of phonons at that temperature. For a given configuration of “frozen” displacements, we calculate the hopping and current matrix elements. The eigenvalues  $\varepsilon_i$  and eigenvectors  $|i\rangle$  of the corresponding Hamiltonian are calculated. For an isotropic system, the optical conductivity is then given by

$$\sigma(\omega) \sim \frac{1}{\omega} \sum_{ij} |\langle i|j_x|j\rangle|^2 (f_i - f_j) \delta(\hbar\omega - \varepsilon_j + \varepsilon_i), \quad (2)$$

where  $f_i$  is the Fermi function for the state  $i$  at temperature  $T$ .

The left insert of Fig. 1 shows that this approach (broken line) agrees quite well with the QMC calculation for large  $T$ , the temperature range we are interested in, and we expect the semiclassical calculation to remain accurate for  $T \gg \omega_{ph}$  ( $= 0.014$  eV). We can therefore interpret the results by analysing the simpler semiclassical calcu-

lation. We observe that this model differs qualitatively from the (Ziman solution [18]) of the Boltzmann equation, in which  $\rho(T) \sim T$  for large  $T$ . In the Boltzmann equation the electrons are treated semiclassically, while here they are treated quantum-mechanically.

Fig. 1 shows that there is a very clear saturation for  $\text{Nb}_3^*$ , while for Nb (right insert) there is only weak saturation at large  $T$ , in agreement with experiment [1,11].

We now discuss the reasons for the saturation. Fig. 2a shows the optical conductivity  $\sigma(\omega)$  for  $\text{Nb}_3^*$  according to the semiclassical theory. For small  $T$ , there is a narrow Drude peak at  $\omega = 0$ , which is smeared out over the whole energy range for large  $T$ . Then  $\sigma(\omega = 0)$  drops correspondingly. However,  $\sigma(\omega)$  remains zero for  $\omega > W$  (apart from a slight broadening introduced in the calculation), where  $W$  is the band width, since there are no excitations for  $\omega > W$ .

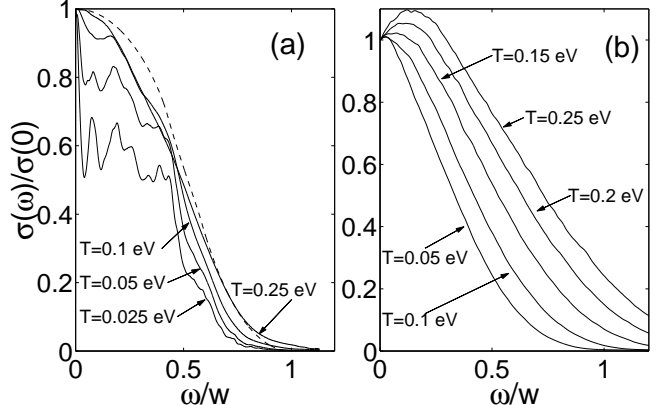


FIG. 2. The optical conductivity as a function of the frequency  $\omega$  for the (a) A15 and (b) fullerene models in the semiclassical calculation. The frequency has been scaled by the  $T = 0$  band width  $W$ . (a) also shows (broken curve) the result of approximating all current matrix elements by their average.

The Drude peak is due to intraband transitions between states with similar values of the wave vector  $\mathbf{k}$ . As  $T$  is raised and the vibrations of the atoms are increased, the states loose their well-defined  $\mathbf{k}$  and band index labels. To illustrate this, we decompose a state  $|i\rangle$  at a finite  $T$  in the  $T = 0$  states with given  $\mathbf{k}$ -vectors and label the weights  $c(i\mathbf{k})$ . We define  $\Delta$  as the average of  $\Delta(i)$  over all states  $i$ , where

$$\Delta(i) = n_{\mathbf{k}} \sum_{\mathbf{k}} c(i\mathbf{k})^2, \quad (3)$$

and  $n_{\mathbf{k}} = 256$  is the number of allowed  $\mathbf{k}$ -vectors for the systems studied. If each state has  $n_{\mathbf{k}}/m$   $\mathbf{k}$ -components with equal weights,  $\Delta = m$ . If periodicity is completely lost,  $\Delta = 1$ , and if each state has only one  $\mathbf{k}$ -component,  $\Delta = n_{\mathbf{k}}$  ( $= 256$ ) [19]. This quantity is shown in Fig. 3. It illustrates how the effects of periodicity are lost very quickly for  $\text{Nb}_3^*$  on a temperature scale of just a few hundred K.

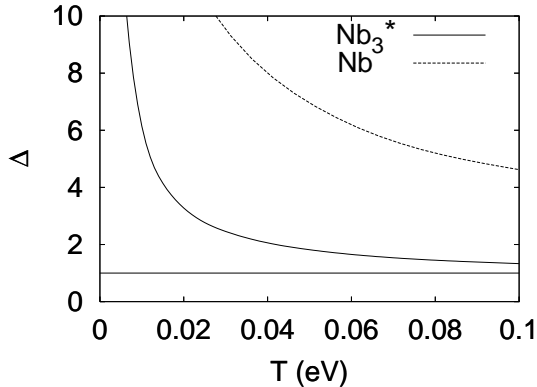


FIG. 3. The measure  $\Delta$  (Eq. (3)) of the amount of momentum conservation as a function of  $T$  for  $\text{Nb}_3^*$  (full line) and  $\text{Nb}$  (dotted line). The horizontal line represents complete loss of momentum conservation.

For a large  $T$ , the  $(\mathbf{q} \rightarrow \mathbf{0})$  current operator then couples all states to each others. We now make the assumption that at large  $T$  the coupling between all states is equally strong [20]. This is the opposite limit to the usual Boltzmann equation treatment, where  $\mathbf{k}$  is still assumed to be a good quantum number. We can then replace a current matrix element in Eq. (2) by its average  $|j_x^{\text{av}}|^2$  over all transitions. Using charge and current conservation (Eq. (1)), we obtain

$$|j_x^{\text{av}}|^2 = \frac{e^2 d^2}{3N^2 n^2} \sum_{\nu\mu} |t_{\nu\mu}|^2 = \frac{e^2 d^2}{3N n^2} \langle \varepsilon^2 \rangle, \quad (4)$$

where  $n$  is the orbital degeneracy and  $\langle \varepsilon^2 \rangle$  is the second moment of the density of states  $N(\varepsilon)$  per atom. We assume some generic shape of  $N(\varepsilon)$ . Since we know its second moment, we can then relate  $N(\varepsilon)$  to the  $j_x^{\text{av}}$ . Using this relation, we can calculate  $\sigma(\omega)$ . The result is shown by the broken curve in Fig. 2a. A comparison with the full calculation illustrates that the approximation of a constant matrix element becomes a good approximation already at moderate values of  $T$ . We find that  $\sigma(0) \sim d^2/\Omega$ , where  $\Omega$  is the volume per atom. Setting  $d$  equal to the  $T = 0$  nearest neighbour distance, we obtain

$$\rho \sim A \frac{d}{n}, \quad (5)$$

where  $n$  is the orbital degeneracy.  $A$  depends on the precise assumptions of the model, but it is  $\sim 0.2$  mΩcm if  $d$  is expressed in Å. Assuming a semi-elliptical density of states  $\sim \sqrt{(W/2)^2 - \varepsilon^2}$ , band filling 0.4 and using the nearest neighbour distance for  $d$ , we find  $A = 0.27$  and  $A = 0.15$  for the A15 and bcc lattices, respectively. This is shown by the broken horizontal lines in Fig. 1. The corresponding  $\sigma(\omega)$  is shown by the broken curve in Fig. 2a. Alternatively, we can calculate  $d$  as  $T$ -dependent average over the neighboring distances, using the hopping

matrix elements as weight factors. This gives the broken almost horizontal lines in Fig. 1. Given the simple assumptions, the agreement with the full semiclassical calculations at large  $T$  is surprisingly good. The corresponding apparent mean-free path is

$$l \sim cn^{1/3}d. \quad (6)$$

With the assumptions above and  $d$  being the nearest neighbour distance, we obtain  $c = 0.5$  and  $c = 0.6$  for the A15 and bcc lattices, respectively. Saturation therefore happens roughly when the Ioffe-Regel condition is satisfied, as might have been expected on dimensional grounds. In deriving Eqs. (5, 6) we have approximated the Fermi functions by theta-functions. Going beyond this approximation would introduce a weak (additional)  $T$ -dependence in Eq. (5).

Eqs. (5, 6) are independent of the band width. A scaling of all  $t_{\mu\nu}$  by a factor  $\alpha > 1$  increases  $W$ , and  $\sigma(\omega)$  is spread out over a larger energy range. At the same time, however,  $j_x^{\text{av}}$  is increased (Eq. (1)) in such a way that  $\sigma(0)$  in Eq. (2) is not changed. Charge and current conservation (Eq. (1)) therefore plays a crucial role for our results Eqs. (5, 6).

The derivation of Eq. (6) relies on a quantum-mechanical treatment of the electrons. It explains why metals with a large resistivity usually show saturation, and why this happens when the apparent mean free path is of the order of the atomic separation.

We next consider the low  $T$  behaviour of  $\rho(T)$ . For  $T > \omega_{ph}$ , we have that [18]

$$\rho(T) = 8\pi^2 \frac{\lambda T k_B}{\hbar \Omega_{pl}^2}, \quad (7)$$

where  $\lambda$  is the dimensionless electron-phonon coupling constant and  $k_B$  is the Boltzmann constant.  $\Omega_{pl}$  is the plasma frequency

$$(\hbar \Omega_{pl})^2 = \frac{e^2}{3\pi^2} \sum_n \int_{Bz} d^3 k \left[ \frac{\partial \varepsilon_{n\mathbf{k}}}{\partial \mathbf{k}} \right]^2 \delta(\varepsilon_{n\mathbf{k}} - E_F). \quad (8)$$

where  $\varepsilon_{n\mathbf{k}}$  is the energy of a state with the band index  $n$  and the wave vector  $\mathbf{k}$  and  $E_F$  is the fermi energy.  $\Omega_{pl}$  depends on the average Fermi velocity.

The straight line given by Eq. (7), and shown in Fig. 1 (chain lines), agrees well with the semiclassical calculations for small  $T$ . Typically, this line rises so slowly that it intersects the horizontal line of Eq. (5) well above the melting point for the metal of interest. Then no saturation is found in the accessible temperature range. If, however,  $\Omega_{pl}$  is small and  $\lambda$  is large, the two lines cross below the melting temperature. We then expect saturation, as is indeed observed. An important difference between  $\text{Nb}_3^*$  and  $\text{Nb}$  is that  $\text{Nb}_3^*$  has many rather flat bands, due to the large unit cell and many forbidden crossings. The resulting small electron velocities, lead to

a small  $\Omega_{pl}$ . We find  $\Omega_{pl} = 3.6$  and 8.2 eV for  $\text{Nb}_3^*$  and Nb, respectively, which makes the slope of the line in Eq. (7) by about a factor of five larger for  $\text{Nb}_3^*$  than for Nb. We find similar  $\lambda$ 's for  $\text{Nb}_3^*$  ( $\lambda = 1.0$ ) and Nb ( $\lambda = 0.9$ ). More accurate estimates give  $\Omega_{pl} = 3.4$  eV ( $\text{Nb}_3\text{Sn}$ ) [21] and 9.5 eV (Nb) [22] and  $\lambda = 1.7$  ( $\text{Nb}_3\text{Sn}$ ) [3] and 1.1 (Nb) [22].

A very different behaviour is found in the alkali-doped fullerenes, ( $\text{A}_3\text{C}_{60}$  ( $\text{A} = \text{K}, \text{Rb}$ )), where the apparent mean free path becomes much shorter than the separations of the  $\text{C}_{60}$  molecules [5,6]. This behaviour was related to the fact that the important (intramolecular) phonons primarily couple to the  $\text{C}_{60}$  level energies, instead of the hopping matrix elements [23,24]. Already at moderate temperatures, the resulting fluctuations in the level energies become comparable to the  $T = 0$  width of the narrow  $t_{1u}$  band, which conducts the current. This leads to the broadening of the  $t_{1u}$  band and of  $\sigma(\omega)$  beyond the  $T = 0$  band width. In contrast to the case of a scaling of the hopping parameters, discussed below Eq. (6), this is, however, not accompanied by an increase of the current operator. Thus  $\sigma(0)$  is reduced, explaining the lack of saturation in this case. This is illustrated in Fig. 2b.

To summarize, guided by the loss of periodicity at large  $T$ , we have studied the effect of replacing the current matrix element by its average. Together with charge conservation, this naturally leads to saturation in systems where the phonons couple to the hopping matrix elements. On the other hand, in models where the phonons couple to the level energies, such as the model for  $\text{A}_3\text{C}_{60}$ , saturation does not happen. The issue of saturation or not saturation is only raised in the experimentally accessible temperature range if  $\lambda$  is large and  $\Omega_{pl}$  is small (see Eq. (7)). This is favoured by the relatively flat bands for  $\text{Nb}_3^*$  ( $\Omega_{pl}$  small) and by the small band width for  $\text{A}_3\text{C}_{60}$  ( $\lambda$  large and  $\Omega_{pl}$  small).

We would like to thank M. Fähnle, O. Jepsen, E. Koch and R. Zeyher for useful discussions, M. Jarrell for making his MaxEnt program available and the Max-Planck-Forschungspreis for financial support.

- [1] Z. Fisk, G.W. Webb, *Phys. Rev. Lett.* **36**, 1084 (1976).
- [2] Z. Fisk, A.C. Lawson, *Solid State Commun.* **13**, 277 (1973).
- [3] P.B. Allen, in *Superconductivity in d- and f-Band Metals* H. Suhl and M.B. Maple, Eds. (Academic, New York, 1980) p. 291.
- [4] A.F. Ioffe, A.R. Regel, *Prog. Semicond.* **4**, 237 (1960).
- [5] A.F. Hebard, T.T.M. Palstra, R.C. Haddon, R.M. Fleming, *Phys. Rev. B* **48**, 9945 (1993).
- [6] J.H. Schön, Ch. Kloc, B. Batlogg, *Nature* **408**, 549 (2000).
- [7] W. Kohn, J.M. Luttinger, *Phys. Rev.* **108**, 590 (1957).
- [8] B. Chakraborty, P.B. Allen, *Phys. Rev. Lett.* **42**, 736 (1979).
- [9] P.J. Cote, L.V. Meisel, *Phys. Rev. Lett.* **40**, 1586 (1978).
- [10] A. Ron, B. Shapiro, M. Weger, *Phil. Mag. B* **54**, 553 (1986).
- [11] J.M. Abraham, B. Deviot, *J. Less-Common Metals* **29**, 311 (1972).
- [12] W.E. Pickett, K.M. Ho, and M.L. Cohen, *Phys. Rev. B* **19**, 1734 (1979).
- [13] E.L. Wolf, *Principles of electron tunnelling spectroscopy* (Oxford University Press, New York, 1985) p. 268.
- [14] W. Harrison, *Electronic structure and the properties of solids. The physics of the chemical bond.* (Dover, New York, 1980).
- [15] O. Jepsen, priv. commun.
- [16] R. Blankenbecler, D.J. Scalapino, R.L. Sugar, *Phys. Rev. D* **24**, 2278 (1981).
- [17] M. Jarrell, J.E. Gubernatis, *Phys. Rep.* **269**, 134 (1996).
- [18] G. Grimvall, *The Electron-Phonon Interaction in Metals* (North-Holland, Amsterdam, 1981) p. 212; 216.
- [19] For  $T \approx 0$ ,  $\Delta \approx 0.1n_{\mathbf{k}} < n_{\mathbf{k}}$  for the clusters considered in Fig. 3, due to mixing of degenerate  $\mathbf{k}$ -states.
- [20] The matrix elements of the current operator actually have a broad distribution of values. However, an average over states with the similar energies, appropriate in Eq. (2), has fairly small variations already at moderate  $T$ .
- [21] L.F. Mattheiss, L.R. Testardi, *Phys. Rev. B* **17**, 4640 (1978).
- [22] S.Y. Savrasov, D.Y. Savrasov, *Phys. Rev. B* **16487** (1996).
- [23] O. Gunnarsson, J.E. Han, *Nature* **405**, 1027 (2000).
- [24] For a strong electron-phonon coupling  $\lambda$ , the  $\rho(T)$  of this model shows some “excess” resistivity at small  $T$ , and a similar model has therefore been used to describe resistivity saturation [25]. This and previous work [23] shows, however, that the model is more appropriate for describing the lack of saturation.
- [25] A.J. Millis, J. Hu, S. Das Sarma, *Phys. Rev. Lett.* **82**, 2354 (1999).